Unilag Journal of Mathematics and Applications,
Volume 4, Issue 1 (2024), Pages 8–20.
ISSN: 2805 3966. URL: http://lagjma.edu.ng

MHD CASSON NANOFLUID FLOW WITH VISCOUS DISSIPATION, CHEMICAL REACTION AND THERMAL RADIATION SUBJECTED TO CONVECTIVE BOUNDARY CONDITIONS

AROLOYE SOLUADE JOSEPH[1], FENUGA OLUGBENGA JOHN [2],
ABIALA ISRAEL OLUTUNJI [3], AND ODESOLA AYOBAMIDELE SUNDAY [4]

Abstract. Casson nanofluid flow in the presence of nanoparticles, viscous dissipation, chemical reactions and thermal radiations under the influence of convective boundary conditions is numerically investigated. Convective conditions of temperature and nanoparticle concentration are employed in the formulation of the problem. The highly governing partial differential equations models the problem are reduced to ordinary differential equations via similarity variables. Numerical solutions via shooting method with six order Runge Kutta scheme used to solve the velocity, temperature and nanoparticle concentration models. The numerical simulation is carried out with the aid of Maple software. The results and influence of embedded flow parameters are presented through graphs and tables. The obtained results are compared with similar existing results in literature and there is excellent agreement. We found that temperature and nanoparticle concentration fields decrease when the values of Casson parameter increases. It is found that the temperature and concentrations fields enhanced as Biots numbers increases due to thermal and concentration convective conditions. The results further revealed that both the thermal and nanoparticle concentration boundary layer thicknesses are higher for the larger values of thermophoresis parameter. It is also observed that temperature and concentrations profiles reduces for large value of Brownian motion parameters. The results further reveal that both the fluid temperature and concentration increases as chemical reaction increases.

1. Introduction

Nanomaterials are introduced as new energy materials because these materials have particles with size as the same as or smaller than the size of de Broglie

2010 *Mathematics Subject Classification.* Primary: 22E30. Secondary: 58J05.
Key words and phrases. Magenetohydrodyamics nanoparticles; Casson fluid; thermal radiations; thermal and concentration convective conditions; chemical reaction.

Submitted: September 23, 2024. Revised: October 23, 2024. Accepted: November 5, 2024.
[1] Correspondence.

wave, Hussain et al. (2015) and Sharma et al. (2009). The use of nanoparticles is now a subject of abundant studies. It is due to their Brownian motion and thermophoresis properties. A new class of heat transfer fluids is known as nanofluids(a base fluid and nanoparticles). The nanoparticles are utilized to enhance the heat transfer performance of the base fluids, Choi and Eastman (1995). The cooling rate requirements cannot be obtained by the ordinary heat transfer fluids because their thermal conductivity is not adequate. Brownian motion of the nanoparticles enhance the thermal conductivity of base fluids. Further, the magnetic nanofluid is a unique material that has properties of both liquid and magnet. The magnetonano-fluid is important for cancer therapy, construction of loud speakers, blood analysis, and etc. Many of physical characteristics of nanofluids can be controlled and adjusted by varying an applied magnetic field. Hosseini and Ghader (2010) provided a model to analyze the viscosity of nanofluid with temperature and particle volume fraction. Kandasamy et a l (2011) investigated the MHD boundary layer flow over a vertical stretching surface in the presence of nanoparticles. They also consider the Suction/blowing effects of their work. They obtained the exact solutions for translational symmetry and numerical solutions for scaling symmetry. Mixed convection flow of nanofluid with magnetic field, suction/injection, viscous dissipation and chemical reaction effects were numerically investigated by Kameswaran et al (2012). Turkyilmazoglu (2012) provided closed form solutions for hydromagnetic thermal slip flow of nanofluid over a linearly stretched surface. Entropy generation analysis in MHD flow of nanofluid was discussed by Rashidi et al (2013). Here, the flow generation is due to the rotation of porous disk. They provided numerical solutions by employing RungeKutta fourth order procedure. Forced convection flow of nanofluid over a horizontal plate was examined by Hatami et al. (2013). Makinde et al. (2013) discussed the buoyancy-driven stagnation point flow of nanofluid over a convectively heated stretching and shrinking surfaces. Hatami and Ganji (2013) investigated the effect of heat transfer in non-Newtonian nanofluid passing the through a porous medium. Hussain et al. (2015) investigated the flow of Casson nanofluid with viscous dissipation and convective conditions: A mathematical model. They implored homotopy perturbation analysis (HAM) as method of solution Boundary layer flows with combined heat and mass transfer over a stretching or moving surfaces are quite essential in many industrial and metallurgical processes. Such situations occur in the design of chemical processing, damage of crops due to freezing, cooling of drying and papers in textile, food processing, cooling towers refrigeration and air conditioning, compact heat exchangers, solar power collectors, cooling of an infinite metallic plate in a cooling bath etc. Various researchers analyzed such flow analysis for different fluid models under isothermal heat and mass conditions, Motsa et al. (2011), Mahmood et al (2013), Turkyilmazoglu (2013), Alsaadi et al (2013), Ferdows et al. (2013). The concept of convective heat condition is quite popular amongst the researchers. Aziz () carried out an analysis to discuss the steady laminar flow over a flat plate with convective boundary condition. Makinde and Aziz (2010) extended the work of Aziz (2009) by considering the MHD flow through a porous medium

with buoyancy force. Makinde and Aziz (2010) also analyzed the variable diffusivity fluid combined with heat and mass transfer in the presence of thermal boundary condition. Three-dimensional boundary layer flow of Jeffery fluid with convective surface condition was discussed by Shehzad et al (2014). Hayat et al. (2013) presented homotopic solutions of buoyancy driven flow of Maxwell fluid near a stagnation point in the presence of convective condition. Boundary layer flow of nanofluid with thermal convective boundary condition was investigated by Makinde and Aziz(2011). Alsaedi et al. (2012) extended the analysis of Makinde and Aziz (2011) by considering stagnation point flow with heat generation/absorption. The present investigation is focused on MHD casson nanofluid flow in the presence of chemical reaction, thermal radiation and viscous dissipation. The problem is subjected to thermal and convective boundary conditions. Further, the Partial differential equation models governing the models are reduced to Ordinary differential equation via similarity variable and the reduced system of equations are solve by shooting method and six order Rung Kutta method. Simulation of the code is carried out using Maple. Graphs and Tables are used to present the numerical results. There is excellent agreement between the obtained results and the similar existing results in literature when compared. We also extend the work of Shahmohamadi (2012), Hayat et al. (2012), Mukhopadhyay (2013), Hussain et al. (2015) to magneto hydrodynamic (MHD) boundary layer flow of Casson nanofluid over an exponentially stretching surface.

2. Problem development

We examine magneto hydrodynamic (MHD) flow of Casson nanofluid over an exponentially stretching sheet in the presence of chemical reactions, thermal radiation and viscouse dissipations. The fluid is taken to be incompressible. We assume that the surface of sheet is heated by a hot fluid with temperature and concentration that give heat and mass transfer coefficients and . Magnetic field of strength is applied normally to the flow. The magnetic Reynolds number is chosen to be small. The induced magnetic field is smaller in comparison with the applied magnetic field and thus neglected. Following Makinde and Aziz (2011), Alsaedi (2012), Shahmohamadi (2012) and Hussain et al. (2015), the MHD boundary layer equations of Casson nanofluid are

$$\frac{\partial u}{\partial x}+\frac{\partial v}{\partial y}=0 \tag{2.1}$$

$$u\frac{\partial T}{\partial x}+\frac{\partial v}{\partial y}=\left(1+\frac{1}{\beta}\right)\frac{\partial^2 u}{\partial y^2}-\frac{\sigma\beta_0^2}{\rho_f}u \tag{2.2}$$

$$\begin{aligned} u\frac{\partial u}{\partial x}+v\frac{\partial T}{\partial y}=\alpha\frac{\partial^2 T}{\partial y^2}+r\left(D_B\frac{\partial C}{\partial y}\frac{\partial T}{\partial y}+\frac{D_r}{T_\infty}\left(\frac{\partial T}{\partial y}\right)^2\right) \\ +\frac{v}{c_p}\left(1+\frac{1}{\beta}\right)\left(\frac{\partial u}{\partial y}\right)^2-\frac{1}{(\rho C)_f}-\frac{\partial q_r}{\partial y} \end{aligned} \tag{2.3}$$

$$u\frac{\partial C}{\partial x}+v\frac{\partial C}{\partial y}=\left(D_B\frac{\partial^2 C}{\partial y^2}\right)+\frac{D_r}{T_\infty}\frac{\partial^2 T}{\partial y}-K(C-C_\infty) \tag{2.4}$$

The boundary conditions for the considered flow analysis are

$$u=u_w(x)=U_0 exp\left(fracxL\right), v=0, -k\frac{\partial T}{\partial y}=h_1\left(T_f-T\right),$$
$$-D_B\frac{\partial C}{\partial y}=h_2\left(C_f-C\right), at, y=0; \tag{2.5}$$
$$u\to, v\to, T\to T_\infty, C\to C_\infty, when, y\to\infty.$$

Where u and v are the velocity components in the and direction; v is the kinematic viscosity; β is the Casson parameter; ρ is the density of fluid; σ is the Steffan-Boltzman constant; α is the thermal diffusivity; $r=\frac{(\rho c)_p}{(\rho c)_f}$ is the ratio of nanoparticle heat capacity and the base fluid heat capacity; v is the kinematic viscosity;c_p is the specific heat capacity; D_B is the Brownian diffusion coefficient; D_I is the thermophoretic diffusion coefficient; k is the thermal conductivity; h_1 and h_2 are the heat and mass transfer coefficients, respectively; T_∞ and C_∞ are the ambient fluid temperature and concentration, respectively, Kr is the constant rate of chemical reactions, q is the radiative heat flux PDE Equations (2.2)-(2.5) is reduced into the dimensionless ODE form by introducing the following new variables:,

$$\eta=y\sqrt{\frac{U_0}{2vL}}exp\left(\frac{x}{2L}\right), u=U_0 exp\left(\frac{x}{L}\right)f'(\eta)$$
$$v=-\sqrt{\frac{vU_0}{2L}}exp\left(\frac{x}{2L}\right),\left(f'(\eta)+\eta f'(\eta)\right)$$
$$Aexp\left(\frac{ax}{2L}\right)\theta(\eta)=\frac{T-T_\infty}{T_f-T_\infty}, Bexp\left(\frac{ax}{2L}\right)\theta(\eta)=\frac{C-C_\infty}{C_f-C_\infty}, \tag{2.6}$$

The equations of linear momentum, energy and concentration in dimensionless form become

$$\left(1+\frac{1}{\beta}\right)f''+f''-2f'^2-M^2f'=0 \tag{2.7}$$
$$\theta^{'}+Prf\theta^{'}+PrNb\theta^{'}\phi^{'}+PrNt\theta^{'2}+PrEc\left(1+\frac{1}{\beta}\right)f^{''2}=0 \tag{2.8}$$
$$\theta^{'}+Lef\theta^{'}+(N_tIN_b)\theta^{'}=0 \tag{2.9}$$
$$f=0, f'=1, \theta^{'}=-Bi_1(1-\theta(0)), \phi^{'}=-Bi_2(1-\phi(0)),$$
$$at, \eta=0, f'\to 0, \theta\to 0, \phi\to 0, as, \eta\to\infty. \tag{2.10}$$

where $M^2=\frac{2\sigma B_0^2 L}{(\rho_j U_0 exp(x/L))}$ is the magnetic parameter $Pr=v/\alpha$ is the prandtl number, $Le=\frac{v}{D_B}$ is the Lewis number; $Nb=\frac{(\rho c)_p D_B(C_f-C_\infty)}{((\rho c)_f v}$ is the Brownian motion parameter; $Nb=\frac{(\rho c)_p D_B(T_f-T_\infty)}{((\rho c)_f vT_\infty}$ is the thermophoresis parameter; $Bi_1=(h_1/k)\sqrt{v/a}, Bi_2=(h_2/D_B)\sqrt{v/a}$ are the Biot numbers. Equation (1.1)

is satisfied identically. The skin friction coefficient, the local Nusselt number and the local Sherwood number are

$$C_j = \frac{r_w}{\rho_f u_w^2(x)}, Nu_x = \frac{xq_w}{k(T_f - T_\infty)}, Sh_x = \frac{xq_m}{D_B(C_f - C_\infty)} \tag{2.11}$$

where r_w is the shear stress along the stretching surface; q_w is the surface heat flux; q_m is the surface mass flux. The local skin-friction coefficient, local Nusselt and local Sherwood numbers in dimensionless forms are given below:

$$\sqrt{2Re_x C_{fx}} = \left(1 + \frac{1}{\beta}\right) f'(0), \sqrt{\frac{2L}{x}} Nu_x / Re_x^{1/2} = -\theta'(0), \sqrt{\frac{2L}{x}} Sh_x / Re_x^{1/2} = -\phi'(0) \tag{2.12}$$

where $Re_x = u_w(x)L/v$ is the local Reynolds number.

3. Discussion of Numerical results

The system of highly nonlinear differential equations (2.7), (2.8) and (2.9) subjected to boundary conditions (2.10) are solved by a numerical approach via shooting method and six-order Runge-Kutta method for different moderate values of the flow, heat and mass transfer parameters. The effective Broyden technique is adopted in order to improve the initial guesses and to satisfy the boundary conditions at infinity. Maple software is used to code and simulate the above numerical procedure. Analysis of variations of Casson parameter β, magnetic parameter M, Prandtl number Pr, Lewis number Le, Biot number Bi_1, thermophoretic parameter Nt, Brownian motion parameter Nb and Eckert number Ec on the dimensionless temperature $\theta(\eta)$ is carried out in figures 18. Figure 1 shows that the temperature and thermal boundary layer thickness decrease for the higher values of Casson parameter. Higher value of Casson parameter corresponds to a decrease in the yield stress that causes a reduction in the fluid temperature and thermal boundary layer thickness. Figure 2 illustrates the effects of magnetic parameter on the temperature. Here, an increase in magnetic parameter leads to an enhancement in the temperature. Physically, larger value of magnetic parameter shows stronger Lorentz force. Such stronger Lorentz force is an agent providing more heat to fluid due to the fact that higher temperature and thicker thermal boundary layer thickness occur. Figure 3 shows that the temperature and thermal boundary layer thickness decrease for higher Prandtl numbers. Prandtl number is the ratio of momentum diffusivity to thermal diffusivity. For higher Prandtl fluids the momentum diffusivity increases while there is decrease in the thermal diffusivity. Here, a decrease in thermal diffusivity dominant is over an increase in the momentum diffusivity. This change in thermal diffusivity shows lower temperature and thinner thermal boundary layer.

TABLE 1. Numerical value of skin-friction coefficient $\left(1+\frac{1}{\beta}\right) f'(0)$ for different values of β and M when compared with Husaain et al. (2015)

		$-\left(1+\frac{1}{\beta}\right) f'(0)$	$-\left(1+\frac{1}{\beta}\right) f'(0)$
β	M	Hussain et al.(2015)	Present Result
0.7	0.5	2.146677	2.14667722
1.2		1.865142	1.86514231
1.6		1.755974	1.75597401
2.0		1.687085	1.68708521
1.2	0.0	1.735577	1.73557701
	0.4	1.819679	1.81967911
	0.7	1.980908	1.98090831
	1.2	2.205917	2.20591723

TABLE 2. Comparison of value of $\theta^{'}(0)$ for different values of Pr with previous existing result $Nt = Nb = 0.0, \beta \to \alpha$ when and $Bi_1 = 1000$ when compared with Makinde And Aziz (2011), Alsaedi et al. (2012) and Hussain et al. (2015)

	$-\theta^{'}(0)$	$-\theta^{'}(0)$	$-\theta^{'}(0)$	$-\theta^{'}(0)$
Pr	Makinde and Aziz (2011)	Alsaedi et al (2012)	Hussain et al (2015)	Present Result
0.07	0.0663	0.0663	0.06637	0.066371
0.20	0.1691	0.1691	0.61913	0.619131
0.70	0.4539	0.4539	0.45395	0.453950
2.00	0.9113	0.9113	0.91132	0.911323

Table 1 presents the numerical value of skin-friction coefficient $-\left(1+\frac{1}{\beta}\right) f'(0)$ for various values of β and M The values of skin-friction coefficient are decreased by increasing β but it increases for higher values of magnetic parameter M. Table 3 shows an excellent agreement with the previous numerical when compared with some existing result in literature

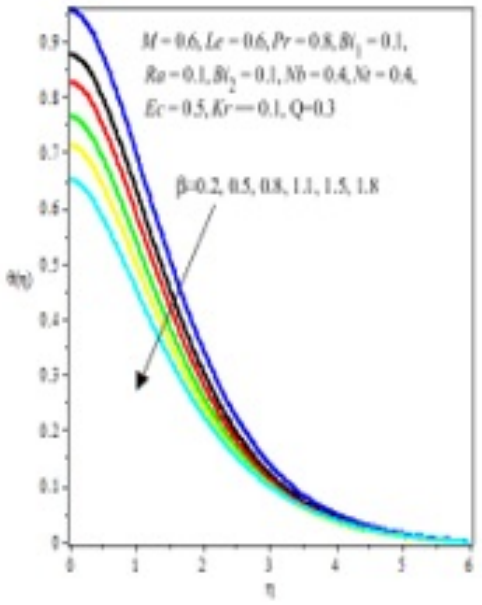

Fig1: Effect of β on Temperature distribution

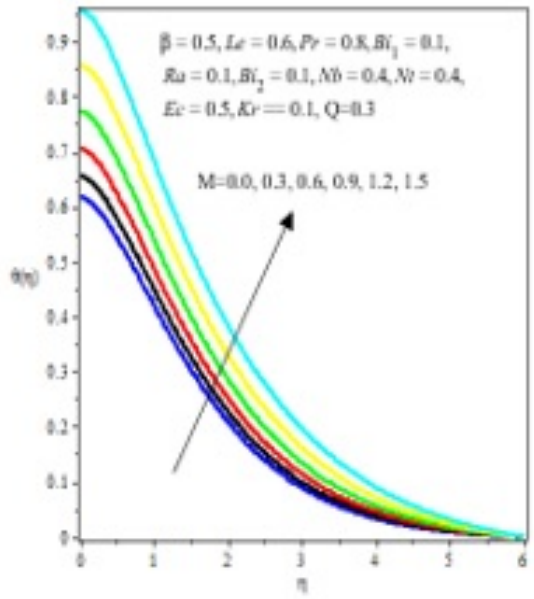

Fig2: Effect of M on Temperature distribution

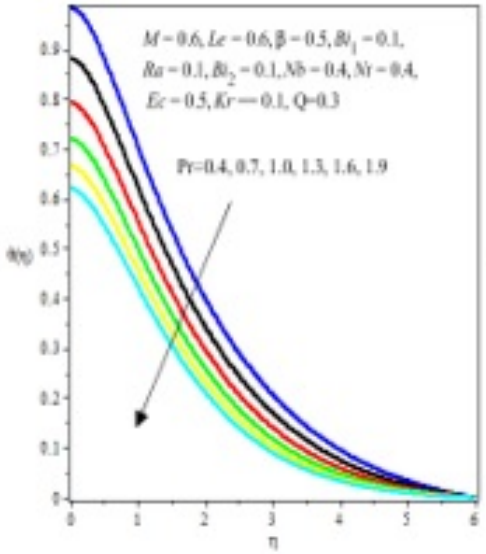

Fig3: Effect of Pr on Temperature distribution

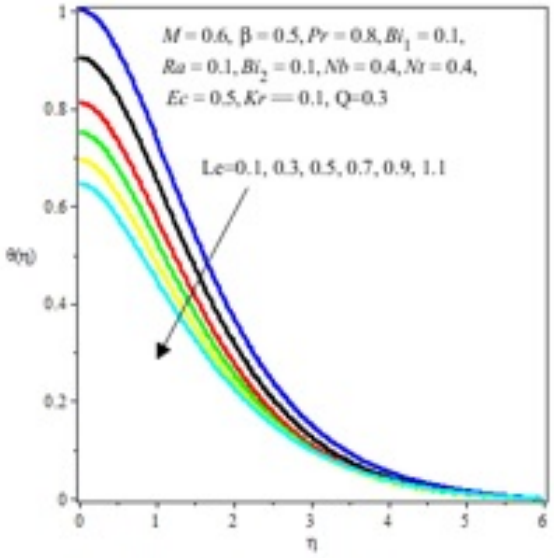

Fig4: Effect of Le on Temperature distribution

The variations in temperature profile for various values of Lewis number are seen in Fig. 4. Temperature increases for smaller values of Lewis number while it increases for higher values of Le. It is known that higher Lewis number fluid has smaller Brownian diffusion coefficient and lower Lewis number fluid has higher Brownian diffusion coefficient. This produces a change in temperature and thermal boundary layer

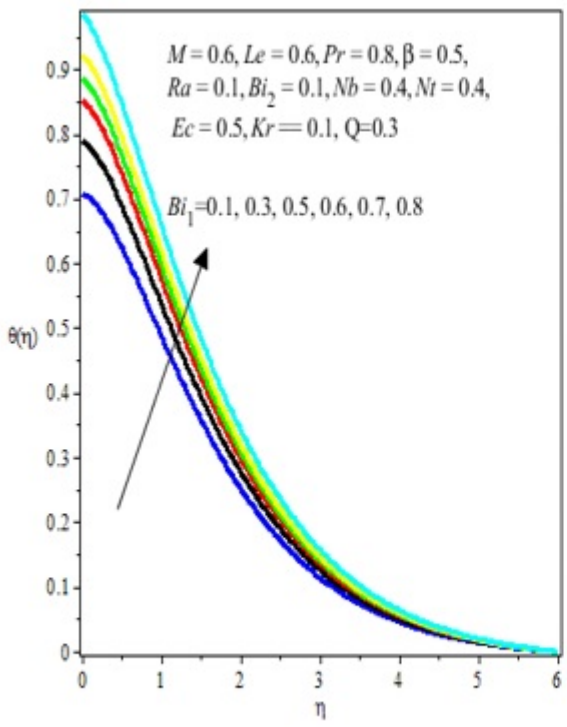

Fig5: Effect of Bi_1 on Temperature distribution

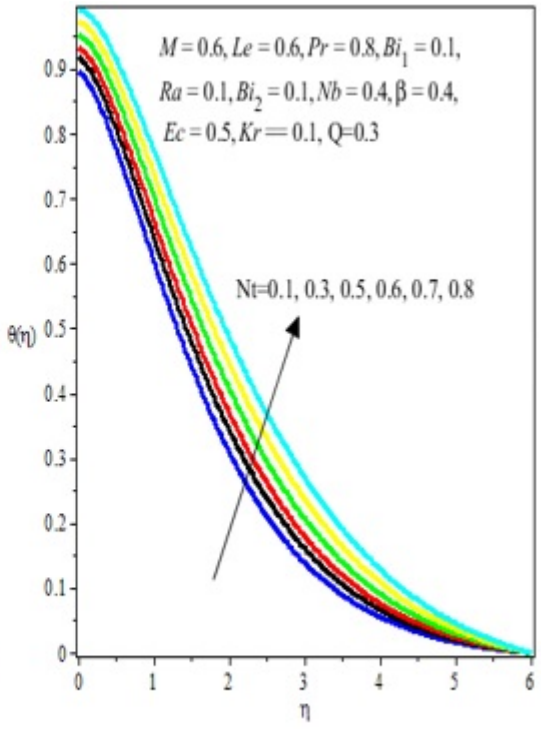

Fig6: Effect of Nt on Temperature distribution

Thickness. Figure 5 depicts the change in temperature profile for different values of Biot number Bi_1 . Temperature increases steadily as Bi_1 increases. Figures 6 and 7 elucidate that both temperature and thermal boundary layer thickness increase through larger thermophoretic and Brownian motion parameters. Figure 8 analyzes that temperature is larger for higher values of Eckert number. Figures 915 are drawn to examine the change in nanoparticle concentration distribution $\phi(\eta)$ for different values of Casson parameter β, magnetic parameter M, Prandtl number Pr, Lewis number Le, Biot number Bi_2 , hermophoretic parameter Nt and Brownian motion parameter Nb.

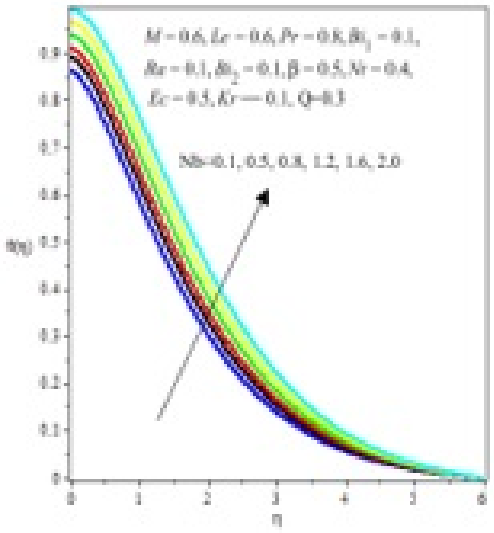

Fig7: Effect of Nb on Temperature distribution

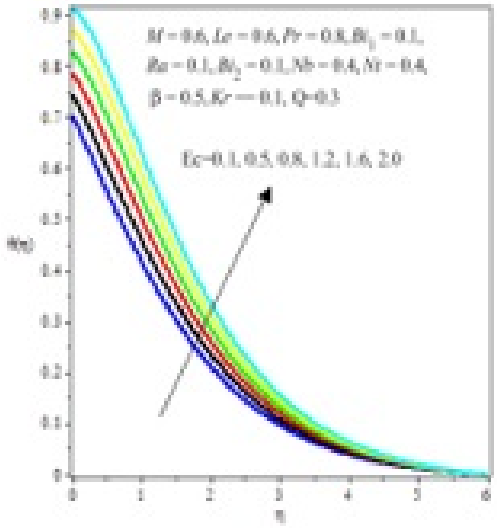

Fig8: Effect of Ec on Temperature distribution

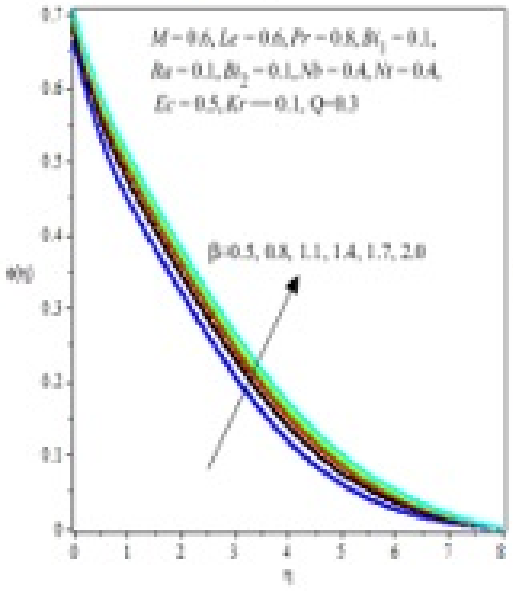

Fig9: Effect of β on concentration distribution

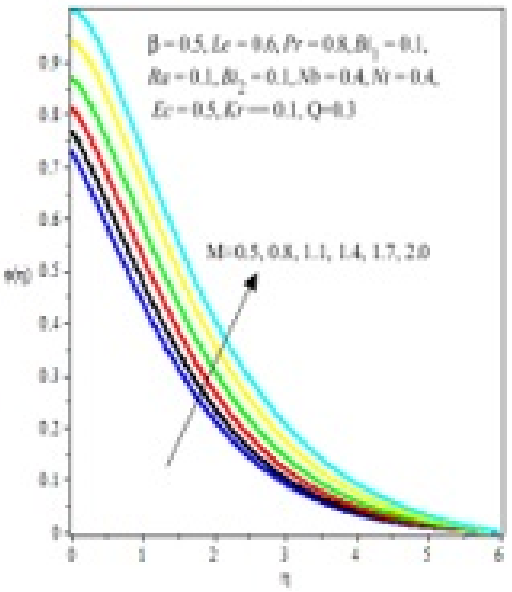

Fig10: Effect of M on Concentration distribution

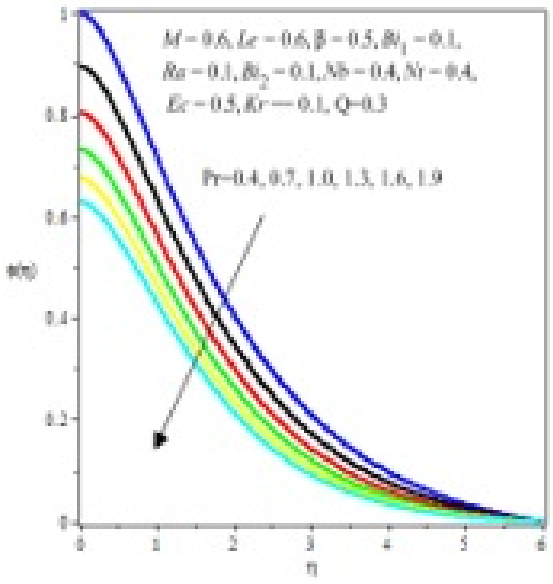

Fig11: Effect of Pr on concentration distribution

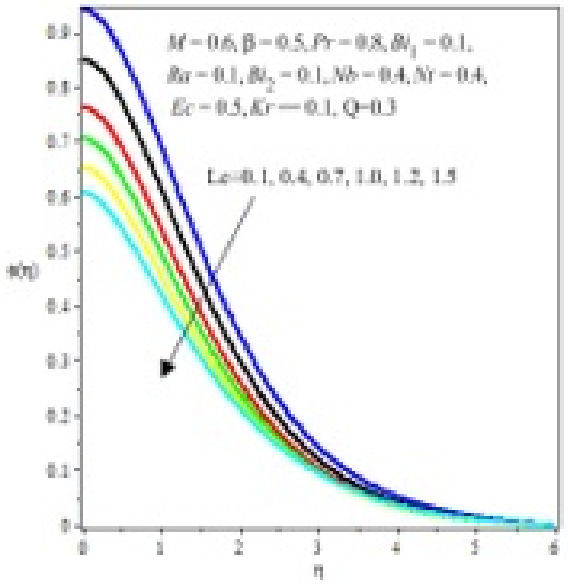

Fig12: Effect of Le on Concentration distribution

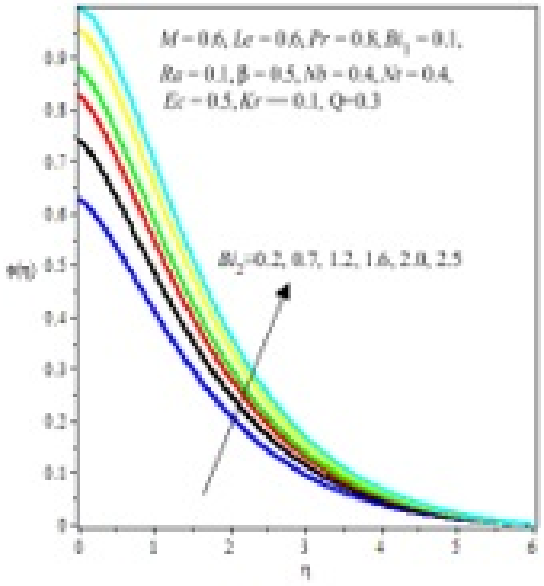

Fig13: Effect of Bi_2 on concentration distribution

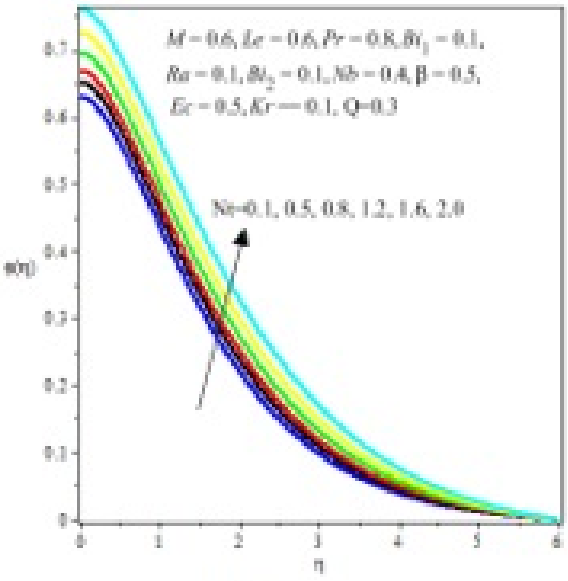

Fig14: Effect of Nt on Concentration distribution

Figures 9 and 10 clearly show that Casson and magnetic parameters have similar effects on the nanoparticle concentration and temperature fields. Figures 11 and 12 indicate that the nanoparticle concentration and its related boundary layer thickness decreases when we increase the values of Prandtl and Lewis numbers. An increase in Biot number Bi_2 gives rise to the nanoparticle concentration profile. Nanoparticle concentration profile increases rapidly as Bi_2 increases but this change in nanoparticle concentration is slow down for higher value of Bi_2 and so on (Fig. 13). In fact, Bi_2 involves the Brownian diffusion coefficient. Brownian

diffusion coefficient increases when we increase the values of Bi_2 . This increase in Brownian diffusion coefficient leads to the higher nanoparticle concentration. Figures 14 and 15 show that the nanoparticle concentration is an increasing function of thermophoretic parameter while on the other hand we observed that the nanoparticle concentration decreases when Brownian motion parameter increases. Figure 15 illustrates that the change in nanoparticle concentration corresponding is more dominant for higher value of Nb. Figure 16 shows the influence of chemical reactions on concentrations profile. Concentration profile increases as chemical reaction increases due to the reaction nano particles in the base fluid

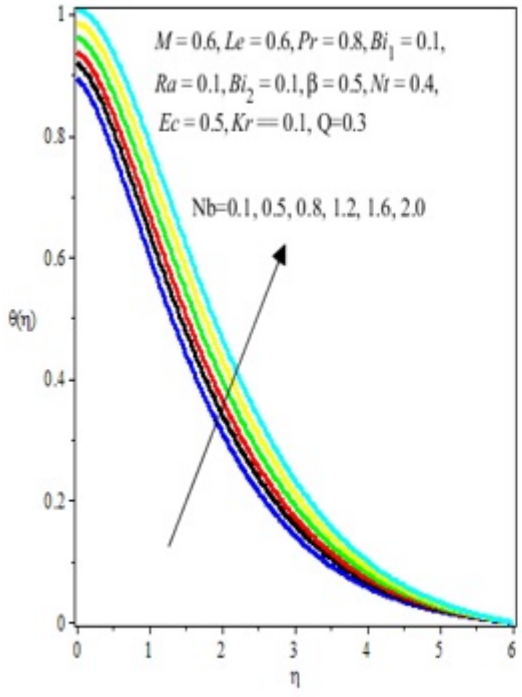

Fig15: Effect of Nb on concentration distribution

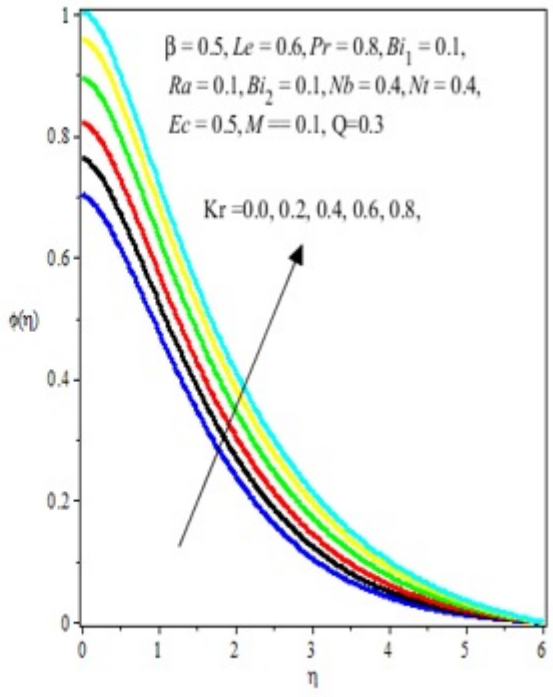

Fig16: Effect of Kr on concentration distribution

4. Conclusions

This research paper focuses on analysis of magnetohydrodynamics Casson nanofluid flow with viscous dissipation, thermal radiation and chemical reaction under the influence of convective boundary conditions.The influence of embedded governing flows parameters are analyses and presented graphically and in tabular. The result revealed that higher value of Casson parameter leads to a decrease in the temperature and nanoparticle concentration. Effects of Lewis number on nanoparticle concentration are more pronounced in comparison with the temperature. Increasing values of Biot numbers Bi_1 and Bi_2 correspond to an increase in the fluid temperature and nanoparticle concentration. Temperature is enhanced for the higher values of thermophoresis and Brownian motion parameters. Effects of thermophoresis and Brownian motion parameters on nanoparticle concentration are quite opposite.

References

[1] T. Hussain, S. A. Shehzad, A. Alsaedi. T. Hayat. M. Ramzan. *Flow of Casson nanofluid with viscous dissipation and convective conditions.* A mathematical model. J. Cent. South Univ. 22: (2015) 11321140

[2] A. Sharma, V.V. Tyagi, C. R. Chen, D. Buddhi. *Review on thermal energy storage with phase change materials and applications.* Journal of Renewable and Sustainable Energy Review, 13: (2009) 318 345.

[3] S. U. S. Choi, J. A. Eastman. *Enhancing thermal conductivity of fluids with nanoparticles.* ASME Internatimal Mechanical Engineering Congress and Exposition. San Francisco, 66: (1995) 99105.

[4] M. Hosseini, S. Ghader. *A model for temperature and particle volume fraction effect on nanofluid viscosity* [J]. Journal of Molecular Liquids, 153: (2010) 139145.

[5] R. Kandasamy, P. Longathan, P. P, Arasu. *Scaling group transformation for MHD boundary-layer flow of a nanofluid past a vertical stretching surface in the presence of suction/injection.* Journal of Nuclear Engineering and Design, 241: (2011) 20532059.

[6] P K. Kameswaran, M. Narayana, P. Sibanda, P. Murthy P. *Hydromagnetic nanofluid flow due to a stretching or shrinking sheet with viscous dissipation and chemical reaction effects.* International Journal of Heat and Mass Transfer, 55: (2012). 75877595.

[7] M. Turkyilmazoglu. *Exact analytical solutions for heat and mass transfer of MHD slip flow in nanofluids* . Journal of Chemical Engineering Science, 84: (2012) 182187.

[8] M. M. Rashidi, N. F Abelman Mehr. *Entropy generation in steady MHD flow due to a rotating porous disk in a nanofluid.* International Journal of Heat and Mass Transfer, 62: (2013) 515525.

[9] M. Hatami, R. Nouri, D D. Ganji. *Forced convection analysis for MHD Al2O3water nanofluid flow over a horizontal plate.* Journal of Molecular Liquids, 187: (2013). 294301.

[10] O D. Makinde, W. A. Khan, Z. H. Khan. *Buoyancy effects on MHD stagnation point flow and heat transfer of a nanofluid past a convectively heated stretching/shrinking sheet.* International Journal of Heat and Mass Transfer, 62: (2013) 526533.

[11] M. Hatami, D. D. Gannji. *Heat transfer and flow analysis for SA-TiO2 non- Newtonian nanofluid passing through the porous media between two coaxial cylinders.* Journal of Molecular Liquids, 188: (2013) 155161.

[12] T. Hussain, S. A Shehzad, A. Alsaedi, T. Hayat, M. Ramzan. *Flow of casson nanofluid with viscous dissipation and convective conditions* A mathematical model. J. Cent. South Univ. 22: (2015) 11321140 DOI: 10.1007/s11771-015-2625-4

[13] S. S. Motsa, S. Shateyi, Z. Mukukula. *Homotopy analysis of free convection boundary layer flow with heat and mass transfer.* Journal of Chemical Engineering Communications 198: (2011) 783795.

[14] M. Mahmood, S. Asghar, M A. Hossain. *Transient mixed convection flow arising due to thermal and mass diffusion over porous sensor surface inside squeezing horizontal channel.* Applied Mathematics and Mechanics: English Edition, 34: (2013). 97112.

[15] M. Turkyilmazoglu. *Heat and mass transfer of MHD second order slip flow.* Journal of Computers and Fluids, 71 (2013) 426434.

[16] F.E. Alsaadi, S A. Shehzad, T. Hayat, S. J. Monaquel. *Soret and Dufour effects on the unsteady mixed convection flow over a stretching surface.* Journal of Mechanics, 2013, 29: (2013) 623632.

[17] M. Ferdows, J. Uddin Md. A. A. Afify. *Scaling group transformation for MHD boundary layer free convective heat and mass transfer flow past a convectively heated nonlinear radiating stretching sheet.* International Journal of Heat and Mass Transfer, 2013, 56: (2013) 181187.

[18] A. A. Aziz. *Similarity solution for laminar thermal boundary layer over a flat plate with a convective surface boundary condition.* Communications in Nonlinear Sciences and Numerical Simulation, 14: (2009) 10641068.

[19] O. D. Makinde, and A. Aziz. *MHD mixed convection from a vertical plate embedded in a porous medium with a convective boundary condition.* International Journal of Thermal Sciences 49: (2010) 18131820.
[20] S. A. Shehzad, T. Hayat, M. S. Alhuthali, S. Asghar. *MHD three-dimensional flow of Jeffrey fluid with Newtonian heating.* Journal of Central South University, 2014, 21: (2014) 14281433
[21] T. Hayat, M. Waqas, S. A. Shehzad, A. Alsaedi. *Mixed convection radiative flow of Maxwell fluid near a stagnation point with convective condition.* Journal of Mechanics, 29: (2013) 403409.
[22] O. D Makinde, A. Aziz. *Boundary layer flow of nanofluid past a stretching sheet with a convective boundary condition.* International Journal of Thermal Sciences, 50: (2011) 13261332.
[23] A. Alsaedi, Awais M, Hayat T. *Effects of heat generation/absorption on stagnation point flow of nanofluid over a surface with convective boundary conditions.* Communications in Nonlinear Sciences and Numerical Simulation, 2012, 17: (2012) 42104223.
[24] H. Shahmohamadi. *Analytic study on non-Newtonian natural convection boundary layer flow with variable wall temperature on a horizontal plate.* Meccanica, 47: (2012). 13131323.
[25] T. Hayat, S. A Shehzad, A. Alsaedi. *Soret and Dufour effects on magnetohydrodynamic (MHD) flow of Casson fluid.* Applied Mathematics and Mechanics: English Edition, 33: (2012) 13011312.
[26] S. Mukhopadhyay, K. Vajravelu, R. A. Van Gorder. *Casson fluid flow and heat transfer at an exponentially stretching permeable surface.* Journal of Applied Mechanics, 80: (2013) 054502.

Aroloye Soluade Joseph [1]
Department of Mathematics, University of Lagos, Akoka, Lagos State, Nigeria.
E-mail address: saroloye@unilag.edu.ng

Fenuga Olugbenga John
Department of Mathematics, University of Lagos, Akoka, Lagos State, Nigeria.
E-mail address: lagjma@unilag.edu.ng

Abiala Israel Olutunji
Department of Mathematics, University of Lagos, Akoka, Lagos State, Nigeria.
E-mail address: liabiala@unilag.edu.ng

Odesola Ayobamidele Sunday
Department of Computer and Mathematics, College of Basic and Applied Science, Mountain Top University, Ogun State, Nigeria.
E-mail address: lagjma@unilag.edu.ng